ARRAYS FOR TENSOR MEASUREMENTS OF THE ELECTRIC FIELD

Aleksandr Mousatov, Mexican Petroleum Institute, Mexico E-mail: amousat@imp.mx
Evgueni Pervago, Mexican Petroleum Institute, Mexico E-mail: epervago@imp.mx
Vladimir Shevnin, Mexican Petroleum Institute, Mexico, E-mail: vshevnin@imp.mx

Abstract

The study of resistivity anisotropy in heterogeneous media is a complex problem that needs developing the special field technology and interpretation technique. Traditional anisotropic resistivity survey requires performing a set of azimuthal measurements. In the case of the anisotropy estimation in heterogeneous media the application of such a technology is essentially restricted by the field-operating complexity for profiling and sounding. On the other hand, at applying the Electrical Resistivity Tomography (ERT) in anisotropic media the neglect of azimuthal–anisotropy influence can result in noticeable errors of interpretation.

The alternative method of anisotropy determination is based on measuring the second derivatives of the electric potential from a point current source. This technology consists in the tensor measurements of the electric field using groups of specially distributed transmitting and receiving electrodes (tensor arrays). The tensor measurements allow obtaining the orientation and value of the resistivity anisotropy from the observations realized for a single orientation of the array without its rotation.

In this report we analyzed the feasibility of different modifications of the tensor array for the determination of anisotropy parameters and their field applicability for profiling and sounding. The sensitivity and stability of the anisotropy estimation with the tensor arrays were shown for a horizontally layered anisotropic medium and vertical anisotropic layer in an isotropic half-space.

Introduction

The geoelectrical investigations in heterogeneous azimuthally - anisotropic media require the special field technology and interpretation because the resistivity measured by Electrical Resistivity Tomography (ERT) method depends on the profile direction. On the other hand anisotropy parameters provide additional important information about geological situation. The determination of the mean resistivity, anisotropy strike and coefficient are based on the circular diagram of apparent resistivity. For this purpose in the point of observation, the apparent resistivity is measured on several azimuths applying the complex field technique with rotation of the whole array (both transmitting and receiving electrodes). The sensitivity of apparent resistivity to anisotropy parameters for the traditional and special type of arrays was studied in (Semenov, 1975, Bolshakov et al., 1997, 1998b). The presence of lateral heterogeneities produces the significant pseudo-anisotropy effect. The separation of the anisotropy and heterogeneity influences can be achieved by performing the modified azimuthal resistivity survey ARS with asymmetrical arrays (Watson and Barker, 1999) and using the spectral analysis of the azimuthal diagrams (Bolshakov et al., 1997, Pervago, Mousatov, Shevnin, 2001).

The time-consuming array rotation can be practically used for measurements in only several points and does not combine with advanced EI technology with a high density of the vertical soundings along profile.

The alternative method of anisotropy–parameters determination based on measuring the second derivatives of the electric potential from a point current source, was proposed in (Mousatov, Pervago, Shevnin, 2000). This technology consists in the tensor measurements of the electric field using specially

distributed groups of transmitting and receiving electrodes (tensor array). The tensor measurements (TENM) allow determining all anisotropy parameters from the observations realized only in one arbitrary direction without array rotation. The stability of the anisotropy estimation with the tensor array of second derivatives in heterogeneous media was tested on 1D models. The application of EI technology with different modifications of the tensor array for the determination of anisotropy parameters above the complex 3D structure with anisotropic basement was presented in (Mousatov, Pervago, Shevnin, 2000).

In this paper we analyze the feasibility of the modified tensor arrays for the horizontally layered and vertically layered structures, which include the azimuthally - anisotropic stratum. The calculation of the measured components of the electric field was based on the analytical solution obtained for the medium composed by anisotropic layers. The performed simulations allow approving the feasibility of tensor arrays for determination of the anisotropy parameters and estimating its stability to the heterogeneity influence as in the case of sounding as for profiling.

Tensor Arrays

The methodology of the tensor measurements was proposed by (Mousatov, Pervago, Shevnin, 2000) and consists in the determination of the second derivatives of the electric potential induced by the point current source S with a group of 9 receiving electrodes $M_{0\text{-}8}$ (Fig. 1).

The system of equations (1-3) for the second derivatives of the potential above a homogeneous anisotropic medium allows determining the anisotropy coefficient λ , the azimuth of anisotropy strike α and the mean resistivity ρ_m.

$$U^{//}_{xx} = \frac{\partial^2 U}{\partial x^2} = \frac{\rho_m}{\pi x^3 \sqrt{\cos^2\alpha + \lambda^2 \sin^2\alpha}}; \quad (1)$$

$$U^{//}_{xy} = \frac{\partial^2 U}{\partial x \partial y} = \frac{\rho_m (\lambda^2 - 1)\cos\alpha \sin\alpha}{\pi x^3 (\cos^2\alpha + \lambda^2 \sin^2\alpha)^{3/2}}; \quad (2)$$

$$U^{//}_{yy} = \frac{\partial^2 U}{\partial y^2} = \rho_m \frac{-\lambda^2 + 2(\lambda^2 - 1)^2 \cos^2\alpha \sin^2\alpha}{2\pi x^3 (\cos^2\alpha + \lambda^2 \sin^2\alpha)^{5/2}}; \quad (3)$$

where: $\lambda = \sqrt{\rho_n / \rho_t}$; $\rho_m = \sqrt{\rho_n \rho_t}$; ρ_t , ρ_n – resistivity values along and across to the anisotropy strike correspondingly, the coordinate origin is in the current source position, the X-axis corresponds to the array axis and Y=0. In the case of heterogeneous media, using these formulas it is possible to define the apparent anisotropy coefficient λ_a, apparent strike angle α_a, and apparent mean resistivity ρ_{am}.

Based on this array we introduced two additional modified tensor arrays (Mousatov, Pervago, Shevnin, 2002).

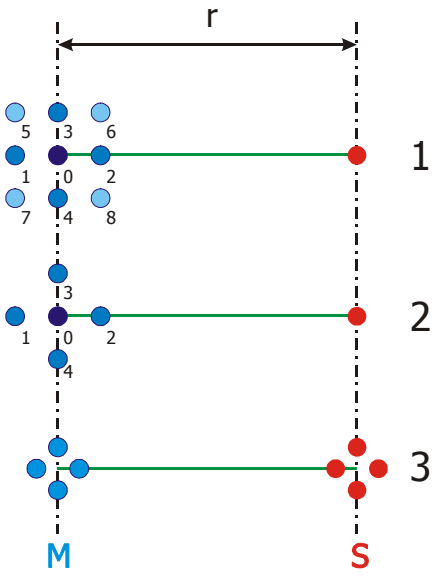

Figure 1.: Arrays for tensor measurements with. 1 - second derivatives; 2 - first derivatives; 3 - mutually perpendicular dipoles

The comparison of the expressions for the second (1-3) and the first derivatives shows that the anisotropy influence on the components U'_x, U''_{xx}, and also U'_y, U''_{xy} is equivalent.

$$U_x^{/} = -\frac{\rho_m}{2\pi x^2 \sqrt{\cos^2\alpha + \lambda^2 \sin^2\alpha}} \qquad (4)$$

$$U_y^{/} = \frac{\rho_m \left(\lambda^2 - 1\right)\cos\alpha \sin\alpha}{2\pi x^2 \left(\cos^2\alpha + \lambda^2 \sin^2\alpha\right)^{3/2}} \qquad (5)$$

Thus the apparent anisotropy parameters also can be determined from the system (3, 4, and 5). The use of the first derivatives allows simplifying the measuring system and diminishing the number of receiving electrodes up to 5 (Fig. 1, 2.). It is necessary to note, that the array for the second and first derivatives is characterized by a high locality of observations and its reference point is in the center of the measuring group.

Since the tensor of the second derivatives of the potential is measured, the proposed method and arrays can be named as tensor measurements and tensor arrays (**TEN**). The tensor array modifications, based on the first and the second derivatives we shall name **TEN**$^{\mathbf{FD}}$ and **TEN**$^{\mathbf{SD}}$ accordingly. Using the array with two mutually orthogonal dipoles, we obtain the next modification of the tensor array - **TEN**$^{++}$ (Fig. 1, 3). In horizontally layered media the **TEN**$^{++}$ and **TEN**$^{\mathbf{SD}}$ arrays are identical, as the derivative in the point of measurement can be exchanged by differentiation in the source point. Such an array can be considered as a combination of axial and equatorial dipole arrays, with additional measurement of the crossed components, similar to the second mixed derivatives of the potential. The apparent anisotropy parameters for the **TEN**$^{++}$ array above inhomogeneous anisotropic media are calculated under the formulas (1-3), where the value of a mixed derivative U_{xy} is accepted equal to half-sum of crossed components measured for each current dipole. The reference point for the **TEN**$^{++}$ array is in the middle point of the array.

Tensor Measurements in Heterogeneous Anisotropic Media

To analyze the feasibilities of tensor array technology for the determination of the anisotropy parameters in heterogeneous media, we simulated the response of the **TEN** arrays for 1D horizontally and vertically layered models that include azimuthally - anisotropic strata. The observation with TEN arrays can be technically realized as for vertical sounding as for profiling.

The vertical sounding with **TEN**$^{\mathbf{FD}}$ and **TEN**$^{\mathbf{SD}}$ requires practically the same field operations as in the case of using the traditional array because the group of measuring electrodes does not move. This circumstance allows applying such tensor array for the electrical tomography with multi channel equipment. Note the difference in the field operation with the azimuthal resistivity survey. When the length of transmitting and receiving line is restricted, the **TEN**$^{++}$ array can be more convenient.

The data obtained with the tensor array in heterogeneous media admit two techniques of quantitative interpretation.

The first approach consists in the separate consideration of the measured potential derivatives. Some components of the electric field can be recalculated into apparent resistivity. The determination of the interpretation model without additional information about the anisotropy presence (the anisotropy coefficient and anisotropy strike) is a serious problem because it should be obtained by integrated analysis of the separate curves, which have complex forms in heterogeneous anisotropic media. The complicate behavior of the apparent resistivity curves for the second derivatives above the azimuthally-

anisotropic heterogeneous media was demonstrated in (Mousatov, Pervago, Shevnin 2000). In this case we need doing the joint inversion of three corresponded functions introducing additionally two parameters related with anisotropy.

The second way consists in calculating the apparent anisotropy parameters (using formulas 1-5): mean resistivity ρ_a, anisotropy coefficient λ_a, and anisotropy strike angle α_a. Based on the apparent mean resistivity it is possible to recognize the structure. The other apparent parameters permit visualization of the anisotropy presence.

We simulated the tensor measurements for the 1D model of piecewise medium with azimuthally - anisotropic layers. The analytical solution for this model was obtained using algorithm published in work (*Bolshakov et al., 1998a*). The results of modeling for the two and tree horizontally layered structures and vertical anisotropic strata are presented below. In these examples the reference point corresponds to the center of the measuring group for the **TEN^{FD}** and **TEN^{SD}** and it is in the middle point of the transmitter-receiver distance for the **TEN^{++}**.

Vertical sounding with the tensor array

The curves of apparent resistivity ρ_a and anisotropy coefficient λ_a calculated for an anisotropic half-space covered with an isotropic overburden with higher and lower resistivity are shown in Fig. 2. These curves reflect adequately the horizontally layered structure with the azimuthally anisotropic basement and weakly depend on the angle between the anisotropy strike and the array direction. In general the character of the apparent mean resistivity is similar to the conventional sounding curve. The asymptotic values of the ρ_a and λ_a graphs tend to the true mean resistivity and anisotropy coefficient accordingly for all azimuths of anisotropy strike (Fig. 2, α=0°, 45°, 90°). We can quantitatively interpret such curves using the traditional methodology of vertical sounding inversion.

To demonstrate the capability of tensor array for the estimation of the true anisotropy direction we presented the apparent anisotropy azimuth α_a and coefficient λ_a as line segments which have length λ_a -1 and its direction indicates α_a (Fig. 3). The accuracy of the determination of the apparent anisotropy azimuth α_a relates with the value of apparent anisotropy coefficient λ_a. When the λ_a is close to 1, the anisotropy azimuth α_a is undefined. The true anisotropy azimuth becomes clear expressed when the spacing exceeds the upper layer thickness in several time.

The curves ρ_a and λ_a for the **TEN^{SD}** array are shifted on right in comparison with the corresponding the **TEN^{FD}** graphs (Fig. 2). The shift is appeared because the depths of investigation for the component U''_{xx} (which used in the **TEN^{SD}**) is about two times lower then for the other the first U'_y, U'_x and the second U''_{yy} derivatives. This discrepancy in the depths of investigation is the reason of a pseudo anisotropy effect that revels on the curves of the apparent anisotropy coefficient.

The influence of pseudo anisotropy on λ_a curves for the **TEN^{SD}** array is illustrated in Fig. 2 where the black curves represent the apparent anisotropy coefficient for the isotropic basement, which has the resistivity equal to the mean resistivity of the anisotropic one. In this case while the λ_a for the **TEN^{FD}** is close to 1 for all spacing, the anisotropy coefficient for the **TEN^{SD}** achieves the maximum value when the spacing is comparable with thickness of upper layer ($L/h \approx 1.5 - 3$). The presence of the pseudo anisotropy effect on the curves λ_a and α_a for the **TEN^{SD}** array explains its distortion and dependence on the anisotropy azimuth for the intermediate spacings (Fig. 2, 3). The discussed effect of pseudo anisotropy is appear on the apparent anisotropy parameters but can be removed if the inversion technique is used for interpretation of data obtained with **TEN^{SD}** array.

The curves of apparent anisotropy coefficient for the **TEN^{FD}** array are free from the pseudo anisotropy effect due to the equal investigation depth of the used components of the electric field.

The considered above features are observed on the apparent parameters' graphs simulated for the three-layer structure (Fig. 4, 5). The intermediate stratum is azimuthally anisotropic (λ=2). The apparent resistivity curves reflect the models and admit the estimation of its characteristic by the standard inversion. The pseudo anisotropy effect related with layering consists in the increasing the influence of anisotropy azimuths on the apparent anisotropy coefficient for the **TEN**^{SD} array.

For example, when the intermediate layer has higher resistivity then the surrounding medium, the apparent anisotropy coefficient for this array has the value about 1.1-1.2, which practically defined by the difference in the depth of investigation and existence of two boundaries with a contrast resistivity changing. The apparent azimuth in this case has no relation with the anisotropy strike orientation and completely depends on the direction of measurements. The estimated azimuth coincides for the L/h=1-10 with the array axis and is perpendicular to this axis for the L/h=10-100 (Fig. 5).

The apparent anisotropy parameters obtained from the **TEN**^{FD} are not affected by the presence of the vertical heterogeneity and allow determining the true anisotropy azimuth for the arbitrary sounding direction despite of the low λ_a value. The maximal value of the apparent anisotropy coefficient has the direct relation with the relative thickness of the anisotropic layer normalized to its depth.

Profiling with tensor array

The diagrams of tensor array profiling above the vertical contact between an isotropic and anisotropic media are presented in Fig.6, 7. The graphs of the apparent mean resistivity for all tensor arrays have a similar behavior as in the case of profiling with the traditional array. The distortion of the ρ_a related with passing of the transmitting and receiving electrodes through the contact is limited by relatively narrow band (in each medium) that corresponds to the array spacing. Outsid60

e of this interval the apparent mean resistivity asymptotically approaches to the true mean resistivity. These curves practically do not depend on the profile orientation outside the distortion zone.

The apparent anisotropy coefficients obtained with **TEN**^{FD} and **TEN**$^{++}$ arrays have the same distortion interval for all profile directions whereas for **TEN**^{SD} this interval decreases when the measuring azimuth becomes close to 90° (Fig. 6). These distortions can be considered as the pseudo anisotropy effect produced by lateral heterogeneity and strongly related with positions of electrodes with respect to contact.

To estimate the area where the apparent anisotropy parameters correspond to true model characteristics we presented the apparent coefficient and azimuth of anisotropy as function of profile orientation (Fig. 7). The length of a line segment is equal to the λ_a-1 value and its orientation corresponds to the α_a. The presented map confirms that the determination of true anisotropy parameters can be realized by using profile data for any measuring direction.

The examples of the apparent parameters simulated for the profile above the vertical azimuthally anisotropic layer surrounded by the isotropic medium are presented in Fig. 8-11. The graphs of the apparent mean resistivity ρ_a and anisotropy coefficient λ_a for the profiling orientation 60° show that the estimation of the true model characteristic can be done when the anisotropic-layer thickness surpasses the array spacing in 3 times (Fig. 8). The apparent parameters for all tensor arrays in the distortion intervals vary significantly and its forms are related with the resistivity ratio between the anisotropic layer and surrounding environment.

The variations of the apparent anisotropy azimuth α_a as function of the measuring directions are illustrated in Fig. 9. The joint presentation of the α_a and λ_a as the map of line segments permits easy detecting the distortion zones and evaluating the anisotropy strike and coefficient.

The distribution of apparent anisotropy parameters using the electrical tomography technology with tensor array was simulated for the model in Fig. 8. The vertical distribution of the α_a and λ_a is

visualized as the cross sections for each type of tensor array in Fig. 10, 11. Based on such images of the anisotropy parameters, it is possible to observe the zones where the apparent parameters correspond to the model anisotropy characteristics. Additionally the distortion zones as function of relative spacing normalized to the layer thickness can be estimated. The comparison of cross sections for different array shows that **TEN**^{SD} array better reflect the anisotropic structure especially when the mean resistivity of the anisotropic layer is lower than resistivity of surrounding environment.

Conclusions

We proposed a new approach to determine the parameters of the azimuthally-anisotropic media by measuring the first, second and mixed derivatives of electric potential with the tensor arrays. The tensor observation allows estimating all anisotropy parameters by performing the measurements at one orientation of the array without its rotation. This advantage of the tensor measurements provides characterizing anisotropy in heterogeneous media. The field operations with the tensor array are compatible with the electrical tomography technology.

The simulation of the tensor measurements for vertically and horizontally layered 1D models demonstrated that the tensor array can be applied for sounding and profiling in azimuthally anisotropic media. The results of observations are presented as the apparent parameters: mean resistivity, coefficient and azimuth of anisotropy. This transformation is stable and the obtained apparent parameters are mutually independent. Such apparent parameters can be analyzed and inverted in true model characteristics by using traditional geoelectrical techniques.

In horizontally layered anisotropic media, the curves of anisotropy coefficient obtained by measuring only second derivatives with **TEN**^{SD} and **TEN**$^{++}$ arrays demonstrate a pseudo anisotropy effect. The influence of layered structure on the apparent anisotropy coefficient is related with the difference in the depth of investigation between radial and tangential second derivatives. The **TEN**^{FD} array is free from the pseudo anisotropy effect produced by layering because in this array the electrical field components with the similar investigation depth are used.

In vertically layered anisotropic media the apparent parameters adequately reflect the structure and anisotropy presence. The apparent parameters for all tensor arrays (as for conventional profiling), tend to the true medium characteristics when the thickness of the azimuthally-anisotropic layer exceeds the array spacing and have distortions related with passing the electrodes through contacts. In such heterogeneous media the apparent anisotropy coefficient for **TEN**^{SD} array has higher resolution and sensitivity to anisotropy.

The selection of array type for the determination of the anisotropy parameters depends on studied structures and field technical conditions. However, the application of **TEN**^{FD} array is more convenient because this array is free from the pseudo anisotropy effect in horizontally layered media, has more investigation depth and it is simpler for the field operation.

When the measurements are performed using the complete measuring electrode arrangement, the apparent anisotropy parameters can be obtained for **TEN**^{SD} and **TEN**^{FD} arrays. In this case the joint analysis of apparent parameters for both tensor arrays allows increasing the reliability of interpretation.

References

1. Bolshakov D.K., Modin I.N., Pervago E.V., Shevnin V.A. Separation of anisotropy and inhomogeneity influence by the spectral analysis of azimuthal resistivity diagrams. *Proceedings of 3rd EEGS-ES Meeting*. Aarhus, Denmark, 1997. P.147-150.

2. Bolshakov D.K., Modin I.N., Pervago E.V., Shevnin V.A. Modeling and interpretation of azimuthal resistivity sounding over two-layered model with arbitrary - oriented anisotropy in each layer. *Proceedings of 60th EAGE Conference*, 1998, Leipzig. P110.
3. Bolshakov D.K., Modin I.N., Pervago E.V., Shevnin V.A. New step in anisotropy studies: arrow-type array. *Proceedings of 4th EEGS-ES Meeting*, Barselona, 1998, p. 857-860.
4. Mousatov A., Pervago E., Shevnin V. New approach to resistivity anisotropic measurements. *Proceedings of SEG 70th Annual Meeting*, Calgary, Alberta, Canada, 2000, NSG-P1.5, 4 pp.
5. Mousatov A., Pervago E., Shevnin V. Anisotropy determination in heterogeneous media by tensor measurements of the electric field. *Proceedings of SEG 72th Annual Meeting*, Salt Lake city. 2002. 4 pp.
6. Pervago E., Mousatov A., Shevnin V. Joint influence of resistivity anisotropy and inhomogeneity on example of a single dipping interface between isotropic overburden and anisotropic basement. *Proceedings of the SAGEEP-2001 conference*. Denver. ERP_7, 10 p.
7. Semenov A.S. Rock anisotropy and electrical fields peculiarities in anisotropic media. *Vestnik of Leningrad University. Ser. Geol. and geography.* 1975. N 24, p.40-47, (In Russian).
8. Watson, K. A. and Barker, R. D, 1999, Differentiating anisotropy and lateral effects using azimuthal resistivity offset Wenner soundings, *Geophysics*, 64, No. 3, p.739-745.

Acknowledgments

The authors consider as the pleasant debt to express gratitude to Instituto Mexicano del Petroleo, where in frameworks of the program “Yacimientos Naturalmente Fracturados” this study was fulfilled.

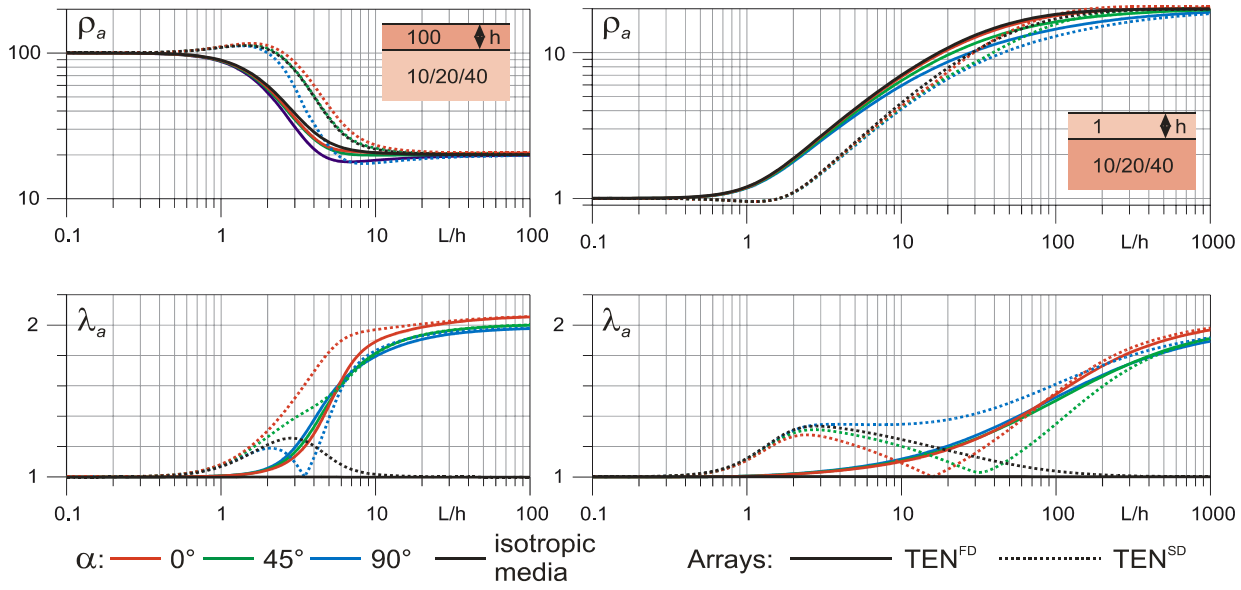

Figure 2.: The curves of apparent mean resistivity ρ_a and anisotropy coefficient λ_a above two-layer structure. The colored curves indicate the true azimuths of anisotropy strike for the anisotropy basement with λ=2. The black graphs correspond to the isotropic basement. The solid curves present the **TEN^{FD}** and dashed ones –the **TEN^{SD}** and **TEN^{++}** arrays.

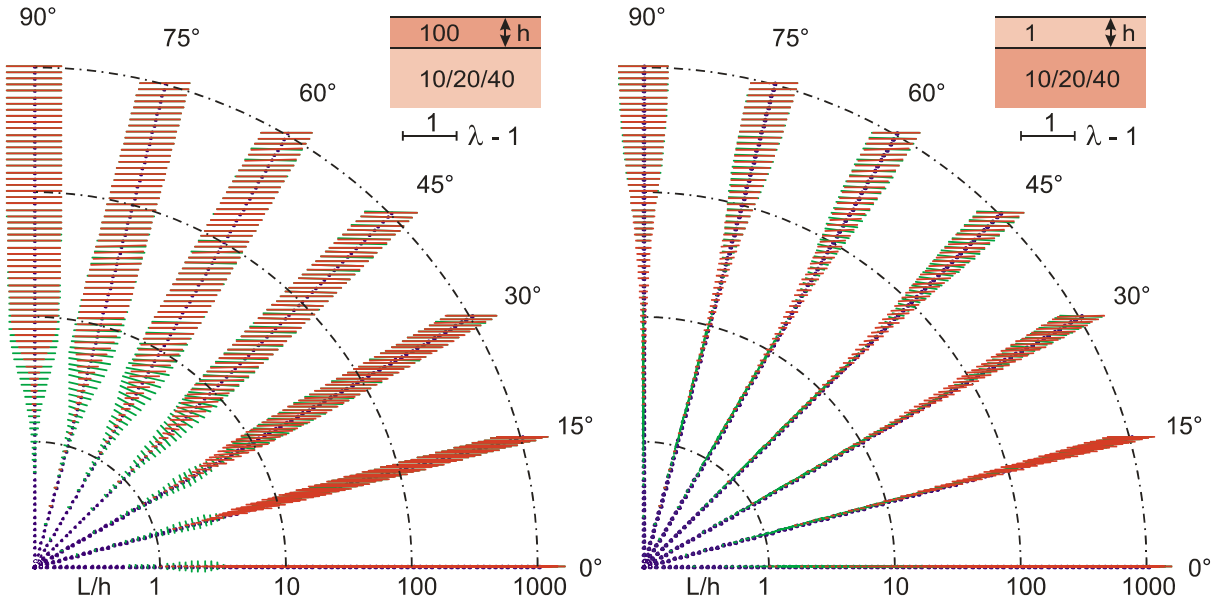

Figure 3.: The apparent anisotropy coefficient λ_a and azimuth α_a as the functions of spacing and orientation of the array axis (two-layer structure). The true azimuth of anisotropy strike is 0°. The anisotropy coefficient of the basement is λ=2. The length and orientation of the line segments is proportional to the λ_a-1 and α_a. The red lines correspond to the **TEN^{FD}** and green ones – to the **TEN^{SD}**.

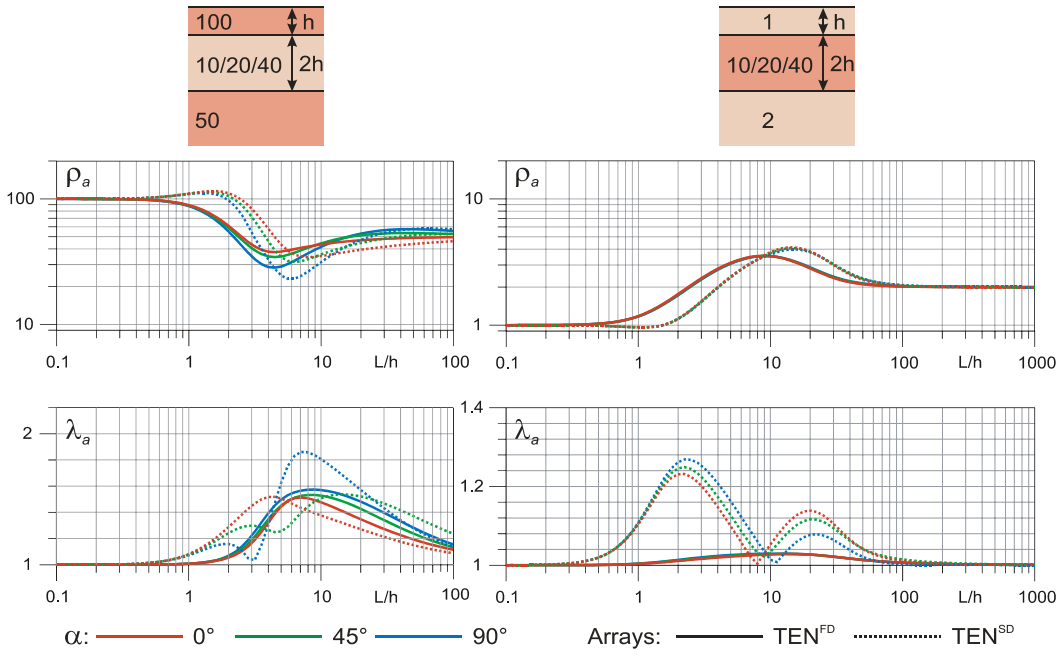

Figure 4.: The curves of apparent mean resistivity ρ_a and anisotropy coefficient λ_a above three-layer structure. The color of curves indicates the true azimuths of anisotropy strike. The anisotropy coefficient of the basement is λ=2.The solid lines correspond to the **TEN^{FD}** and green ones – to the **TEN^{SD}** and **TEN^{++}**.

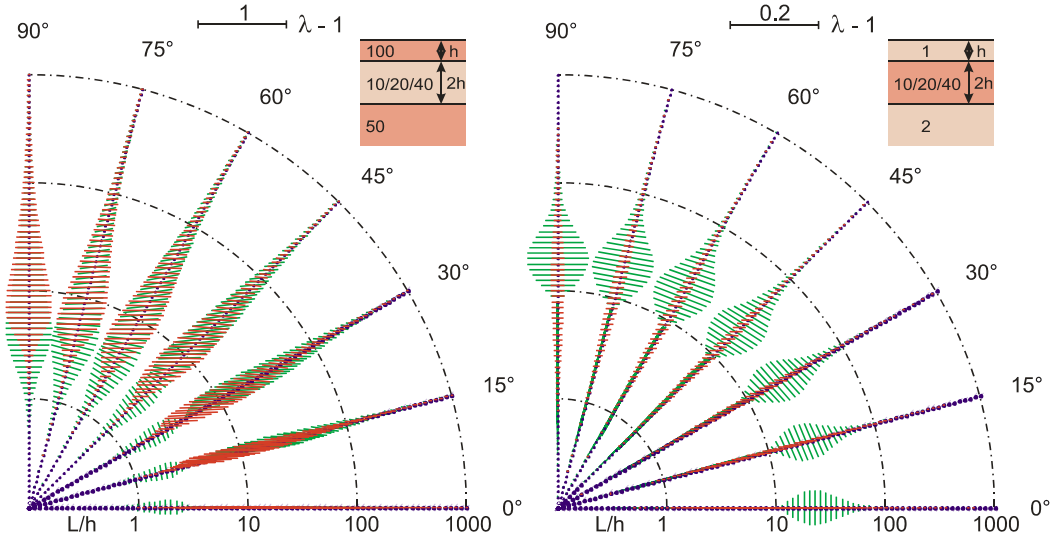

Figure 5.: The apparent anisotropy coefficient and azimuth as the functions of spacing and orientation of the array axis (three-layer structure). The true azimuth of anisotropy strike is 0°. The anisotropy coefficient of the intermediate layer is λ=2. The length and orientation of the line segments is proportional to the λ_a-1 and α_a. The red lines correspond to the **TEN^{FD}** and green ones – to the **TEN^{SD}**.

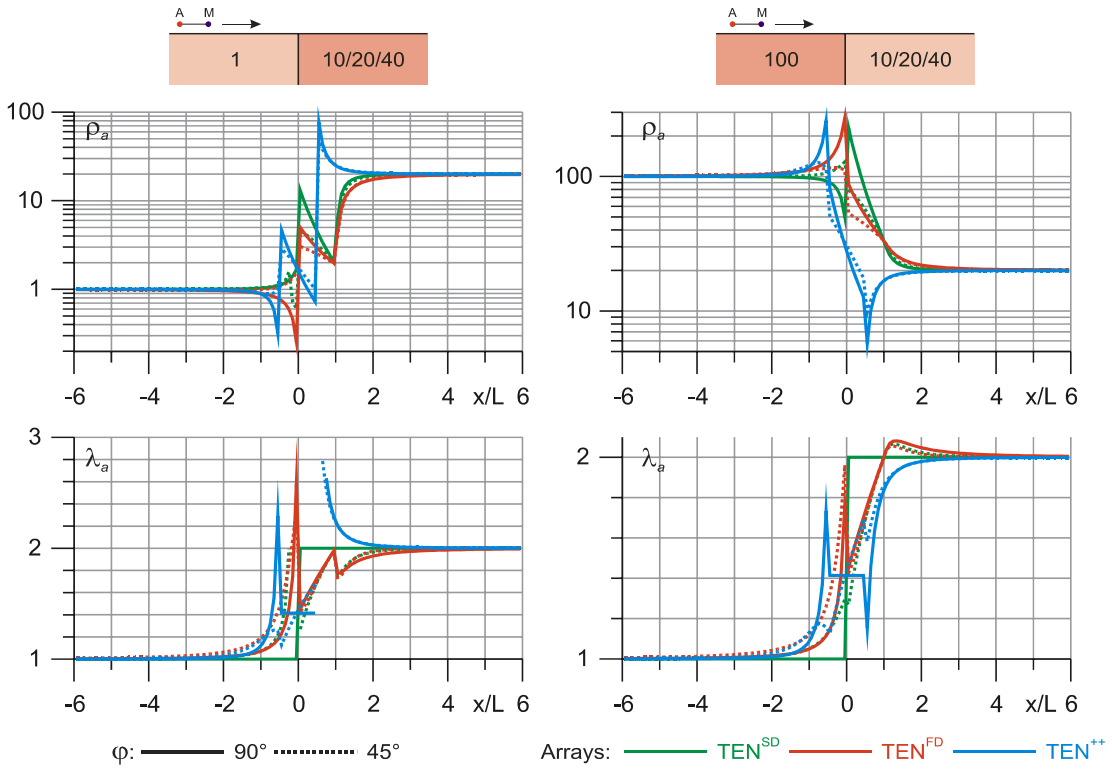

Figure 6.: The profiling curves of the ρ_a and λ_a above the vertical contact between the isotropic and anisotropic (λ=2) half-spaces. The anisotropy strike is in a parallel to the contact (α=0°). The profile directions with respect to the contact plane are φ=90° (solid line) and φ=45° (dashed line). L is the array spacing.

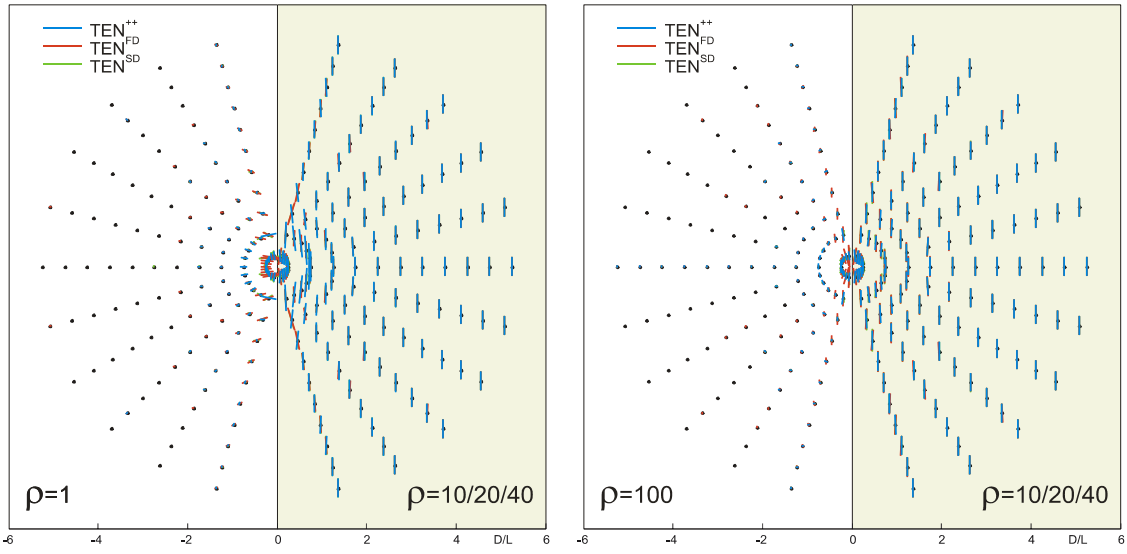

Figure 7.: Map of the α_a and λ_a vs. the profile orientation above the vertical contact between isotropic and azimuthally anisotropic (λ=2) half-spaces. The anisotropy strike is in a parallel to the contact (α=90°). The length of a line segment is equal to the λ_a-1 value and its orientation corresponds to the α_a.

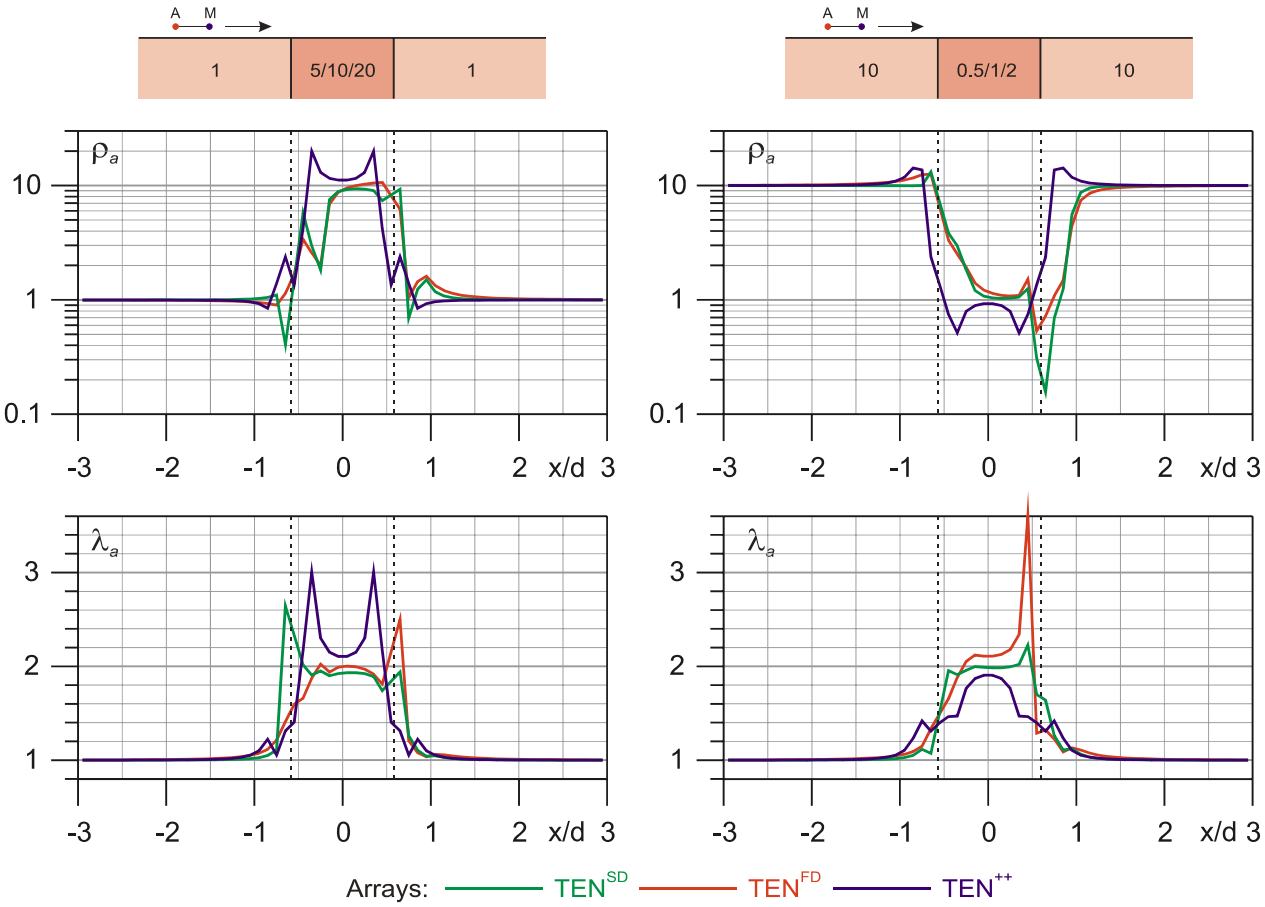

Figure 8.: The profiling curves ρ_a and λ_a above the vertical anisotropic (λ=2) layer placed in the isotropic medium. The anisotropy strike is in a parallel to the contact (α=0°). The profile direction with respect to the layer strike is φ=60°. The array spacing is the L/3h. The dashed vertical lines are the effective layer thickness along the profile direction.

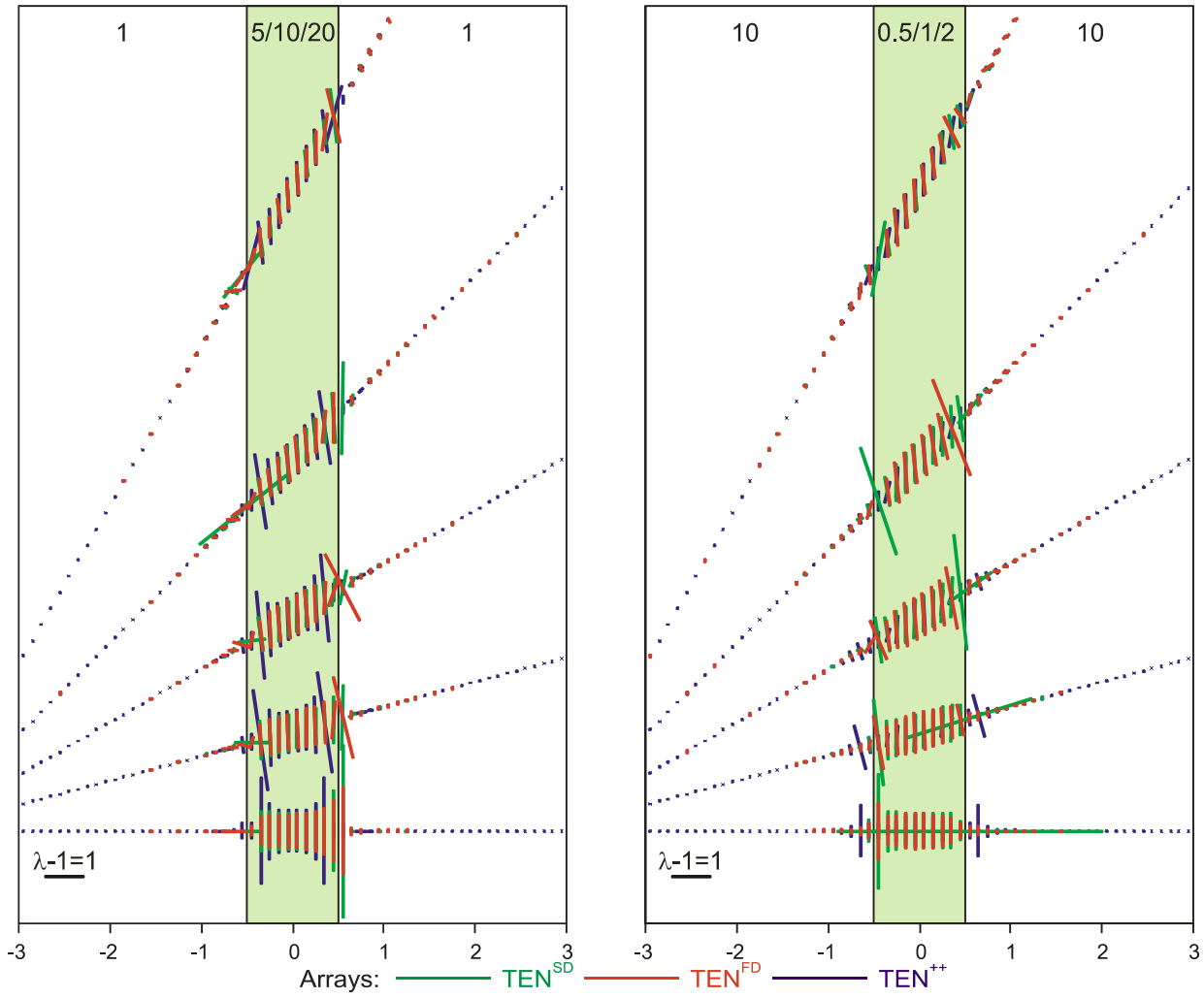

Figure 9.: The apparent azimuth α_a and anisotropy coefficient λ_a vs. the profile orientation φ above the structure presented in the Fig. 8. The length of a line segment is equal to the λ_a-1 value and its orientation corresponds to the α_a. The array spacing is the L/3h.

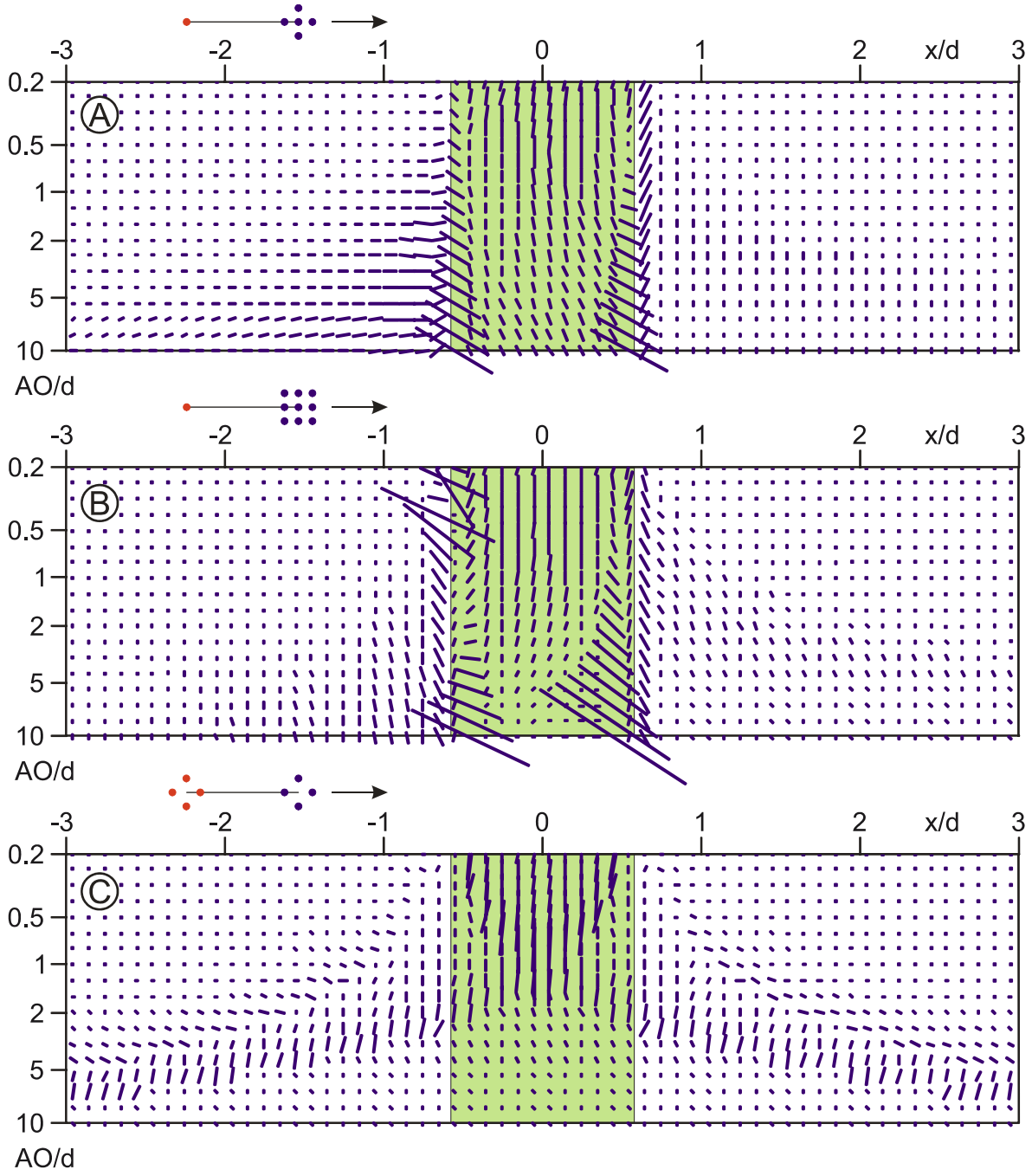

Figure 10.: The cross sections of the apparent azimuth α_a and anisotropy coefficient λ_a above the structure presented in the Fig. 8 with higher mean resistivity of the anisotropic layer. The length of a line segment is equal to the λ_a-1 value and its orientation corresponds to the α_a. The profile orientation φ=60°.

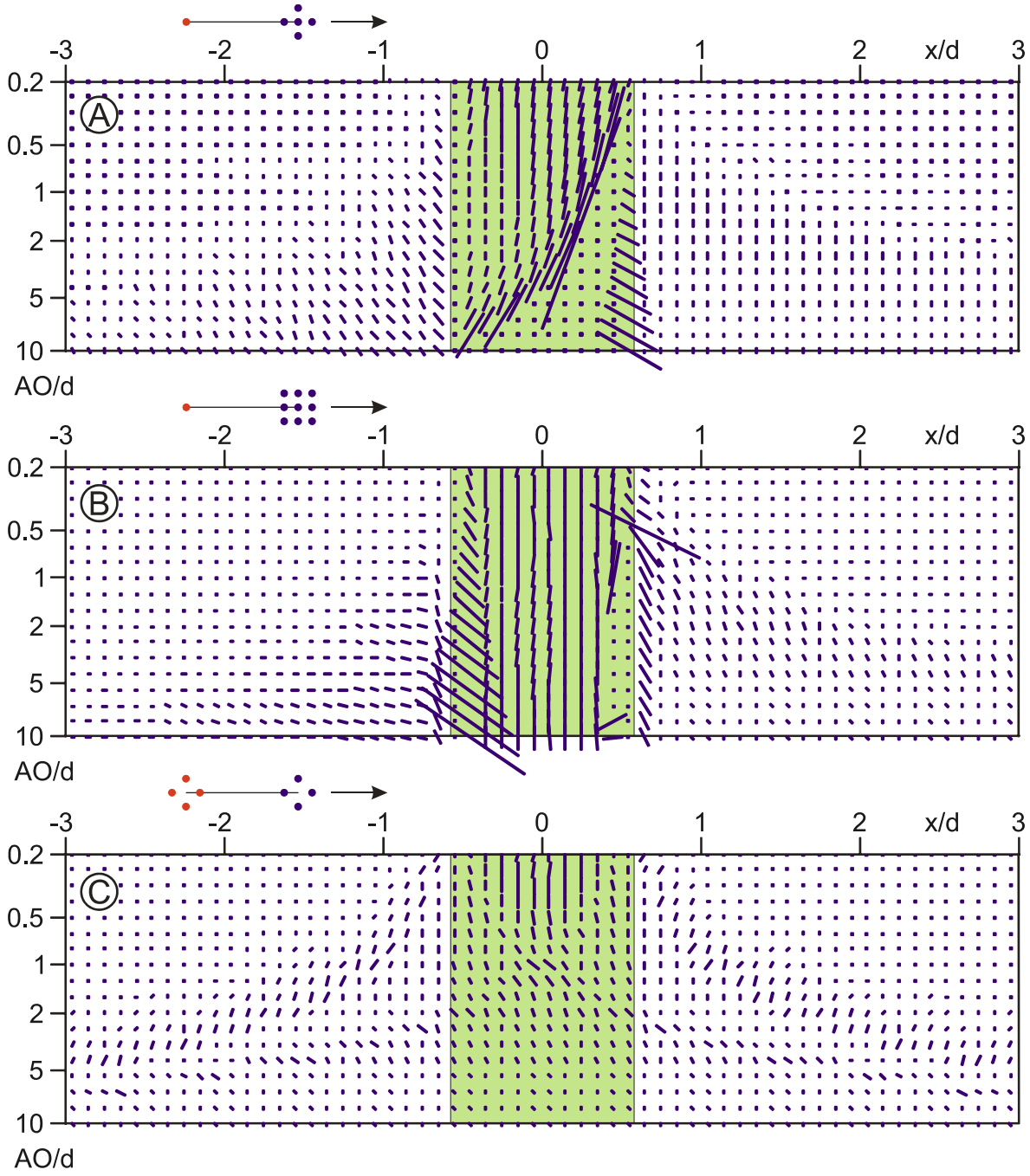

Figure 11.: The cross sections of the apparent azimuth α_a and anisotropy coefficient λ_a above the structure presented in the Fig. 8 with lower mean resistivity of the anisotropic layer.The length of a line segment is equal to the λ_a-1 value and its orientation corresponds to the α_a. The profile orientation φ=60°.